Design of an Autonomous Humanoid Robot

Gordon Wyeth, Damien Kee, Mark Wagstaff, Nathaniel Brewer,

Jared Stirzaker, Timothy Cartwright and Bartek Bebel

School of Computer Science and Electrical Engineering

University of Queensland

St. Lucia, Queensland, 4072

Australia

Abstract

This paper describes the design of an autonomous humanoid robot. The robot itself is currently under construction, however the process of designing the robot has revealed much about the considerations for creating a robot with humanoid shape. The mechanical design is a complete CAD solids model, with specific motors and transmission systems selected. The electronic design of a distributed control system is also complete, along with the electronics for power and sensor processing. A high fidelity graphical simulator has been developed, providing important early feedback on critical design decisions.

1 Introduction

There are several reasons to build a robot with humanoid form. It has been argued that to build a machine with human like intelligence, it must be embodied in a human like body. Others argue that for humans to interact naturally with a robot, it will be easier for the humans if that robot has humanoid form. A third, and perhaps more concrete, reason for building a humanoid robot is to develop a machine that interacts naturally with human spaces. The architectural constraints on our working and living environments are based on the form and dimensions of the human body. Consider the design of stairs, cupboards and chairs; the dimensions of doorways, corridors and benches. A robot that lives and works with humans in an unmodified environment must have a form that can function with everyday objects. The only form that is guaranteed to work in all cases is the form of humanoid.

1.1 The *GuRoo* Project

The *GuRoo* project in the University of Queensland Robotics Laboratory aims to design and build a 1.2m tall robot with human proportions that is capable of balancing, walking, turning, crouching, and standing from a prostrate position. The target mass for the robot is 30 kg, including on-board power and computation. The robot will have active, monocular, colour vision and vision processing.

The intended challenge task for the robot is to play a game of soccer with or against human players or other humanoid robots. To complete this challenge, the robot must be able to move freely on its two legs. It requires a vision sense that can detect the objects in a soccer game, such as the ball, the players from both teams, the goals and the boundaries. It must also be able to manipulate and kick a ball with its feet, and be robust enough to deal with legal challenges from human players. Clearly, the robot must operate in a completely autonomous fashion without support harnesses or wiring tethers.

These goals are yet to be realised for the GuRoo project. Currently the robot exists as a complete mechanical CAD model (see Figure 1), a complete electronic model and a high fidelity dynamic simulation. The dynamic simulation has been programmed to crouch, jump and balance. The progress to this stage has revealed much about the design considerations for a humanoid robot.
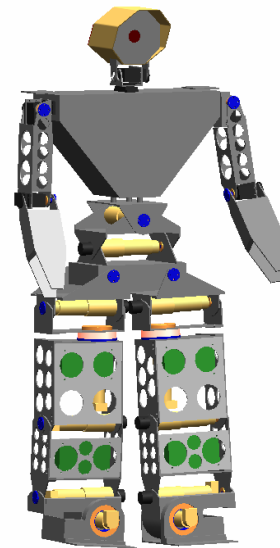

Figure 1: Full CAD model of the GuRoo humanoid robot.

1.2 Paper Overview

This section has described the motivation for building a humanoid robot, and the specific challenge that has been set for the GuRoo project. The subsequent section will

look at other humanoid robot projects, including bipedal walking robots.

The rest of the paper describes the mechanical, electronic and software design of the GuRoo robot. In particular, the paper will detail the mechanical model of the robot and a comparison to the human form, the motors and sensors, the complete electronic design, a full dynamic software simulation of the robot, the software architecture of the robot, and results for balancing and crouching in simulation.

2   Prior Art

2.1   Bipedal Walking Robots

Research into bipedal walking robots can be split into two categories: *active* and *passive*. The passive or un-powered category (for example, McGeer's passive dynamic walker [McGeer, 1990]) is of interest as it illustrates that walking is fundamentally a dynamic problem. Passive walkers do not require actuators, sensors, or computers in order to make them move, but walk down gentle slopes generating motion by the hardware geometry. The passive walkers also illustrate the walking can be performed with very little power input.

Active walkers can further be split into two categories; those that employ the natural dynamics of specialised actuators, and those that are fully power operated. Raibert [Raibert, 1986] and later Pratt [Pratt, 1998] have shown some impressive feats of walking and gymnastic ability in robots that have the capacity for energy storage in the actuator. These robots have been shown to have robust and stable performance from relatively simple control mechanisms.

The alternate approach is to control the joints through pre-specified trajectories to a known "good" gait pattern (for example, [Golden, 1990]). This is a simple approach, but lacks robustness to disturbances. This approach becomes more complex when additional layers are added to provide adjustments to the gait for disturbance. Controlling a fully powered biped in a manner that depends on the dynamic model is complicated by the complex dynamic equations for the robot's motion. Yamaguchi et al. [Yamaguchi, 1998] moved a dynamic torso with significant mass through 2 DOF to keep the Zero Moment Point (ZMP) within the polygon of the support foot. This approach contributed to successful control of the robot, but produces an awkward gait.

2.2   Bipedal Walking Humanoid Robots

There are few examples of autonomous biped walkers that resemble the structure of a human. The Honda company biped robots, P2 and P3 are two of the few examples of such robots [Hirai, 1998]. P3 can walk on level ground, walk up and down stairs, turn, balance, and push objects. The robot is completely electrically and mechanically autonomous. The Sony SDR-3X robot is another example with similar capabilities, although details of the design are yet to be published.

3   Mechanics

The mechanical design of the humanoid requires careful and complex tradeoffs between form, function, power, weight, cost and manufacturability. For example, in terms of form, the robot should conform to the proportions of a 1.2m tall human. However, retaining the exact proportions compromises the design in terms of the selection of actuation and mechanical power transmission systems. Affordable motors that conform to the dimensional restrictions have insufficient power for the robot to walk or crouch. This section describes the final mechanical design and how the balance between conflicting design requirements has been achieved.

3.1   Proportions

The target proportions for the robot are based on biomechanical data of the human form. Figure 2 shows the proportions of the frontal plane dimensions of a 50th percentile male based on data from a United States survey [Dempster, 1965]. The dimensions shown in millimetres indicate the appropriate sizes of anatomical features when scaled to a total height of 1200 mm against the comparable dimensions on GuRoo.
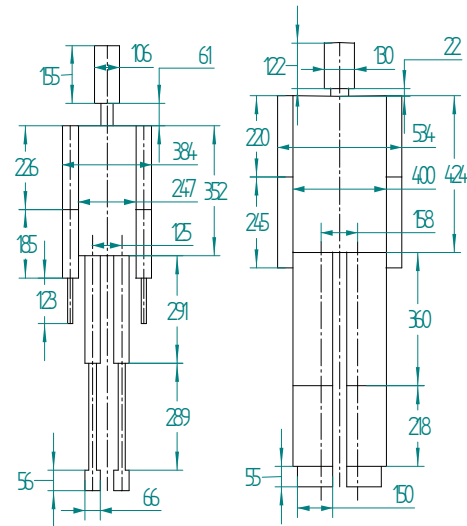

Figure 2: The proportions of typical human anatomy compared to the matching proportions of GuRoo's anatomy. The dimensions indicate the sizes for a human scaled to 1.2m in height.

By comparison, GuRoo is somewhat thickset in the legs, as was dictated by the form of the chosen actuators (see Section 3.3). The spacing between the hips and ankles has been retained, rather than placing the hips and ankles along the frontal centreline of each leg. Our simulation studies showed that the required torques around the roll axes of the hips and ankles becomes excessive if the hips and ankles are spaced too far apart (see Section 5.3).

The body and upper leg of GuRoo are somewhat longer than the counterparts in the human model. This is due to the chain of actuators required for three degrees of freedom in the waist and hips respectively (see Section 3.2). Consequently, the lower leg and the neck and head are shorter to compensate. The overall effect is still convincingly human-like in shape.

The changes in volume required to house the

actuators, as well as the mass of the actuators themselves have an effect on the mass distribution. Table 1 shows the mass distribution of GuRoo compared to that of a human. The most notable exception is that the shin and foot are much heavier in GuRoo than the human counterpart, due to the mass of the powerful actuators required in the ankle. The arms are significantly lighter than the human counterpart, as they are significantly inferior in power and do not have hands. GuRoo's mass distribution is closer to the human distribution than either MIT's active bipedal walker [Paluska, 2000], or McGeer's passive dynamic bipedal walker.

Table 1: Comparison of GuRoo mass distribution with human mass distribution, and with the mass distribution of MIT's M2 bipedal walker and McGeer's passive dynamic walker.

Body Component	GuRoo mass (kg)	GuRoo	Human	M2	PDW
Head and Upper torso	7.3	24%	31%	0%	0%
Abdomen and Hips	9.1	30%	27%	51%	50%
Thigh	5.8	19%	20%	22%	30%
Shin and Foot	6.4	21%	12%	27%	20%
Arm	1.9	6%	10%	0%	0%
Total	30.5				

The other notable point from Table 1 is the total mass of the robot. A 1.2 m tall human would typically be a child approaching his or her 7th birthday, with a 50th percentile mass of 23 kg. A child with mass of 30.5 kg at the same age would be in 97th percentile, indicating that GuRoo is somewhat overweight.
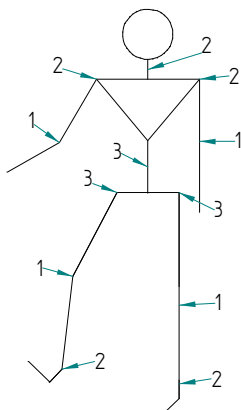
3.2 Architecture

Figure 3: The location of the joints in GuRoo, indicating the degrees of freedom in each joint.

The extent to which human joint function can be replicated is another key factor in robot design. Figure 3 shows the degrees of freedom contained in each joint area of the robot. In the cases where there are multiple degrees of freedom (for example, the hip) the joints are implemented sequentially through short links rather than as spherical joints. Other key differences to the human form are the lack of a continuous flexible spine, and the

lack of a yaw axis in the ankle. Another point to note is that the roll and pitch axes of the ankle are orthogonal, whereas the human ankle has an angle of about 64° between the roll and pitch axes.

3.3 Motor Choice

The key element in driving the mechanical design has been the choice of actuator. The robot has 23 joints in total. The legs and abdomen contain 15 joints that are required to produce significant mechanical power, most generally with large torques and relatively low speeds. The other 8 joints drive the head and neck assembly, and the arms. The torque and speed requirements are significantly less. Factors of cost, weight and availability limited the choice of actuators to rotary DC motors

The 15 high power joints all use the same motor-gearbox combination. The motor is a Maxon RE 36 wound for a nominal voltage of 32V. This motor can provide 88.5 mNm of torque continuously, with a matching current consumption of 1.99 A. The motor has a maximum permissible speed of 8200 RPM. The gearbox has a reduction of 156, with an efficiency of 72%. The maximum continuous generated output torque is 10 Nm, with a maximum output speed of 51 RPM, or 5.3 rad/s. The thermal limits of the motor permit intermittent output torque of up to 19Nm. Each motor is fitted with an optical encoder for position and velocity feedback. The total mass of the motor/gearbox/encoder unit is 0.85 kg.

The 8 low power joints are Hi-Tec RC servo motors model HS705-MG. These motors have an integrated gearbox and have rated output torque to 1.4 Nm, at speeds of 5.2 rad/s. These also have potentiometer feedback and built-in control and power electronics. They require 6V power, and a pulse width modulated signal to indicate desired position. The mass of each unit is 0.125 kg.

4 Electronics

A distributed control network controls the robot, with a central computing hub that sets the goals for the robot, processes the sensor information, and provides coordination targets for the joints. The joints have their own control processors that act in groups to maintain global stability, while also operating individually to provide local motor control. The distributed system is connected by a CAN network. In addition, the robot requires various sensor amplifiers and power conversion circuits.

4.1 Computing

4.1.1 Central Hub

The central control of the robot derives from a hub of three heterogeneous microprocessors that provide coordination between joints, integrate sensor information, and process the vision input. This hub also provides communication to the outside world through user interfaces and communication peripherals.

The primary component of the central controller is an iPAQ pocket pc from Compaq. The iPAQ features a 208 MHz StrongARM microcontroller, 32 Mb of RAM

and a 320 x 240 colour screen. The screen is touch sensitive allowing stylus input of text and graphics. The iPAQ has 16 Mb of Flash ROM to store the operating system. The iPAQ in the GuRoo operates with Windows CE. As well as the touch screen interface, the iPAQ is equipped with a speaker and microphone, a joypad, and four push-buttons. It has an infra-red interface for external communication.
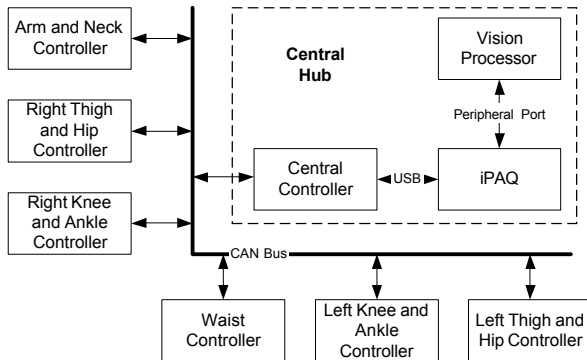

Figure 4: Block diagram of the distributed control system.

The second component of the central hub is a TMS320F243 microcontroller that acts as an adapter and filter for the robot's internal CAN network (see Section 4.1.3). The microcontroller communicates with the robot's distributed control system through the CAN network, and to the iPAQ through the iPAQ's USB serial communication port. The microcontroller also manages the power supply (see Section 4.2.3) providing centralised control of the robot power supply in the event of system failure. This microcontroller is the same device used in the joint controllers (see Section 4.1.2).

The final component of the central is the vision processing board. This board has been developed for the ViperRoos robot soccer team [Chang, 2001] and features a 200 MHz Hitachi Super-H SH4 microcontroller, an FPGA-based programmable camera and bus adapter, 16 Mb of RAM, 8 Mb of flash ROM, and 512 kb of fast SRAM for video caching. The board interfaces to the 100 pin parallel peripheral bus on the iPAQ to provide real time visual display on the iPAQ's colour screen. The vision input comes from a custom digital CMOS camera, based around the OV7620 camera chip from OmniVision, which can provide 640 x 480 images at up to 25 fps. The camera can provide data in YUV or RGB formats, and can be programmed to only send data from selected areas of the sense region.

4.1.2 Joint Controllers

The TMS320F24x series is a 32 bit DSP designed for motor control. The availability of the Control Area Network (CAN) module in this series, along with bootloader programmable internal Flash memory makes the device particularly attractive for this application. Furthermore the device features 8k words of internal flash memory, 8 PWM channels with deadband generation, quadrature input circuitry, an 8 channel 10 bit analog to digital converter with a conversion time of 800ns, a power drive protection external interrupt, and a 50ns instruction time. The TMS320F241 from Texas Instruments operates at 20MHz, and can read the A/D converter, calculating a PID control law, current limit, and generate the required PWM output, in under 10 ?s [Wyeth, 2001]. In this application, we use the TMS320F243, which has an external bus that is used for attaching additional sensor interfaces. Five controller boards control the 15 high power motors, each board controlling three motors. A sixth controller board controls the eight RC servo motors.

4.1.3 Internal Network

The CAN bus is a highly reliable standard developed by Robert Bosch GmbH for use in the automotive environment. It is a multi-master system, with sophisticated error checking and arbitration, so that any high priority message will always get through first without corruption by other messages. All data contained in each packet (up to eight bytes) is also checked with a Cyclic Redundancy Check (CRC) error-checking scheme that can correct up to five random errors, and will be automatically retransmitted if not correct. The network operates at up to 1 Mbit/sec.

4.2 Power

4.2.1 Drive Power Electronics

The drive power electronics is based on a switch mode power stage, requiring only a single supply rail and having an efficiency over 90%. This efficiency results in several advantages such as small size, lower cost power devices and less heatsinking. The H-Bridge channels are driven from separate PWM outputs of the DSP, allowing the deadband features of the PWM peripheral to be used, along with the immediate (<12ns) shutdown of these pins in the event of a fault which triggers the Power Drive Protect Interrupt (PDPInt) pin on the DSP.

A integrated solution was chosen for this design – the SGS-Thomson L6203. This device uses low on-resistance and fast switching MOSFETs, to give maximum efficiency and best control. The voltage limit of the devices is 48V, and the total continuous RMS current limit is 4A. This is a good match to the chosen motors and batteries. The total on-resistance of the power devices is 0.3? . The cost of the device is low, compared to a discrete solution, and the volume and mass of the electronics is minimised by the choice of an integrated solution.

4.2.2 Battery Packs

The power for the 15 high power motors is provided by 4 x 1.5Ah 42V NiCd packs. These packs are effectively paralleled to a common bus (see Section 4.2.3). The packs are chosen to give 20 minutes of continuous operation. The power for the 8 low power motors is derived from a single 3Ah 7.2 V NiCd battery pack. The power for the control electronics is derived from a second single 3Ah 7.2V NiCd pack. The voltage from this pack is distributed to the various boards that require power where it is regulated locally.

4.2.3 Power Regulation

Connecting NiCd batteries in parallel can be extremely hazardous to the life of the batteries. Uneven charging and discharging characteristics between packs can lead to uneven load sharing and high current circulation between

packs. The power from each pack is controlled through switch mode buck converters to provide even current sharing between packs, providing a voltage bus at marginally below the lowest battery voltage.

4.3 Sensing

4.3.1 Joint Sensing

Current sensing is performed in the high power joints by a 0.01Ω resistance in the ground leg of the H-Bridge. The voltage from these sense resistors is amplified by differential amplifiers and measured by the ADC. Current is also checked against a screwdriver adjustable hard limit that is used to trigger the Power Drive Protect interrupt. The position feedback from the encoders on the high power joints provides a count on every edge of both quadrature channels. This provides 2000 counts per motor revolution from the 500 count encoder wheels. In addition, each DSP can measure the bus voltage, and the temperatures of the MOSFETs and motors.

4.3.2 Motion Sensing

In addition to the sensing in each joint, and of course the visual feedback, the robot features 2 x 2-axis accelerometers to provide information about the torso's dynamic behaviour and the relationship to the vertical gravity force. While it is impossible to resolve the motion components of the body's acceleration from the effects of gravity, these sensors may be able to provide information with regard to disturbances while walking – playing a similar role to the human middle ear.

5 Software

The software consists of four main entities: the global movement generation code, the local motor control, the low-level code of the robot, and the simulator. The software is organised to provide a standard interface to both the low-level code on the robot and the simulator. This means that the software developed in simulation can be simply re-compiled to operate on the real robot. Consequently, the robot needs a number of standard interface calls that are used for both the robot and the simulator. Figure 5 shows modularisation of the software, and the common interfaces.
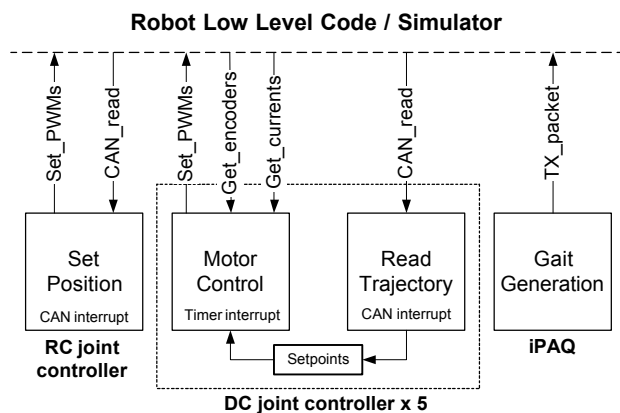

Figure 5: Block diagram of common software modules and the interface used to both the real robot and the simulator.

5.1 Simulator

At present, all evaluations of the robot have taken place in a high fidelity dynamic simulator. The simulator is based on the *DynaMechs* project [McMillan, 1995]. DynaMechs is an object-oriented, open source code library that provides full dynamic simulation for tree-structured robots having a star topology. The algorithms are capable of simulating fixed and mobile bases. The library is based on efficient recursive algorithms for the dynamic calculations, and provides graphical display of the robot in an OpenGL environment.

The simulator uses the DynaMechs package as the core, with additions to simulate specific features of the robot such as the DC motors and motor drives, the RC servos, the sensors, the heterogeneous processing environment and the CAN network. These additions provide an identical interface between the dynamic graphical simulation and the controller and gait generation code. The parameters for the simulator are derived from the CAD models and the data sheets from known components. These parameters include the modified Denavit-Hartenberg parameters that describe the robot topology, the tensor matrices of the links and the various motor and gearbox characteristics associated with each joint. The surface data from the CAD model is also imported to the simulator for the graphical display.

The simulator uses an integration step size of 500μs and updates the graphical display every 5ms of simulated time. When running on 1.5 GHz Pentium 4 under Windows 2000, the simulation updates all 23 joints at a very useable 40% of real time speed.

5.2 Joint Controller Software

For the high power DC motor joints, the simulator provides the programmer with readings from the encoders and the current sensors, based on the velocities and torques from the dynamic equations. In the case of the RC servos, the simulator updates the position of the joints based on a PD model with a limited slew rate. The programmer must supply the simulator with PWM values for the motors to provide the control. The simulator provides fake interrupts to simulate the real events that are the basis of the control software.

There are two types of joint controller boards used in the robot – five controller boards control the fifteen high power motors and one controller controls the eight low power motors. The controller software for the low power motors is a single interrupt routine that is triggered by the arrival of a CAN packet addressed to the controller's mailbox. The routine reads the CAN mailbox for the change in position sent by the gait generation routine. The PWM duty cycle that controls the position of the RC servos is varied accordingly.

The control loop for the high power controllers has two interrupt routines. As for the low power controller, an interrupt is executed upon receipt of trajectory data in the CAN mailbox. The data is used to set the velocity setpoints for the motor control routine. There is also a periodic interrupt every 500 μs to run the motor control software. The motor control routine compares the error between velocity setpoint and the encoder reading and generates a PWM value for the motor based on a

Proportional-Integral control law. The routine also checks the motor current against the current limits, and adjusts the PWM value to prevent over-current situations.

5.3 Motion Generation Software

To this point, the software for motion generation has been used to test the designed geometries and chosen motors in the simulator. The software uses only local joint feedback; it does not use feedback from the joint sensors in a global sense or use the motion sensors to modify the motion to maintain balance. The tests are run without current limiting in the local control loop to evaluate worst-case performance.

The first test motion is a crouch with a return to the standing position. This test has been designed to evaluate the required torques in the pitch joints of hip, knee and ankle. The worst-case results for the knee joint are shown in Figure 6. The second test motion is a lean to balance over one leg, designed to evaluate the required torques in the roll joints of hip and ankle. The joints are driven according to the following equations. The worst-case results for the ankle are shown in Figure 7. In both of these worst cases, the current consumption only briefly exceeds the continuous current rating, and the motor stays within thermal limits.
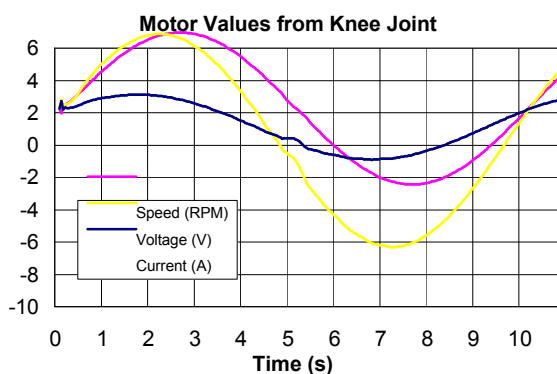

Figure 6: Simulation results for knee motor during a squatting movement. The movement cycle time is 10 seconds.
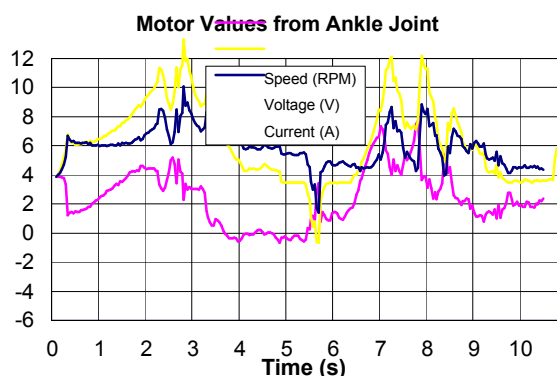

Figure 7: Simulation results for ankle motor during a balancing movement. The movement cycle time is 10 seconds.

6   Conclusions

This paper has illustrated the design of a practical, affordable, autonomous, humanoid robot. The robot is well proportioned in relation to the human form, with most of the major degrees of freedom of the human body implemented. The robot design has a distributed control design with processors dedicated to each of the key roles around the robot. Investigations of the CAD design using a high fidelity simulation have shown that robot is capable of crouching and balancing.

References

[Chang, 2001] M. Chang, B. Browning and G. Wyeth. ViperRoos 2000. RoboCup-2000: Robot Soccer World Cup IV. Lecture Notes in Artificial Intelligence 2019. Springer Verlag, Berlin, 2001.

[Dempster, 1965] W.T.Dempster and G.Gaughran. Properties of body segments based on size and weight. American Journal of Anatomy,1965.

[Golden, 1990] J. A. Golden and Y. F. Zheng. Gait Synthesis For The SD-2 Biped Robot To Climb Stairs. International Journal of Robotics and Automation 5(4). Pages 149-159, 1990.

[Hirai, 1998] K. Hirai, M. Hirose, Y. Haikawa, and Takenaka. The Development of Honda Humanoid Robot. IEEE Conference on Robotics and Automation, 1998.

[Hodgins, 1995] J. K. Hodgins, W. L. Wooten, D. C. Brogan, and J. F. O'Brien. Animating Human Athletics. In Computer Graphics, (Siggraph 1995).

[McMillan, 1995] S. McMillan, Computational Dynamics for Robotic Systems on Land and Underwater, PhD Thesis, Ohio State University, 1995.

[McGeer, 1990] T. McGeer. Passive Dynamic Walking. International Journal of Robotics Research, 9(2):62-82, 1990.

[Paluska, 2000] D.J. Paluska, Design of a Humanoid Biped for Walking Research, Masters Thesis, MIT, 2000.

[Pratt, 1998] J. Pratt and G. Pratt. Intuitive Control of a Planar Bipedal Walking Robot. IEEE Conference on Robotics and Automation, 1998.

[Raibert, 1986] M. H. Raibert. Legged Robots that Balance. MIT Press, Cambridge, MA, 1986.

[Wyeth, 2001] Wyeth G.F., Kennedy J. and Lillywhite J. (2000) Distributed Digital Control of a Robot Arm, Proceedings of the Australian Conference on Robotics and Automation (ACRA 2000), August 30 - September 1, Melbourne.

[Yamaguchi, 1998] J. Yamaguchi, S. Inoue, D. Nishino, and A. Takanishi. Development of a Bipedal Humanoid Robot Having Antagonistic Driven Joints and Three DOF Trunk. Proceedings of the 1998 IEEE/RSJ Conference.